Deactivation of Hydrodesulfurization Catalysts by Metals Deposition

Primary causes of deactivation of hydrodesulfurization catalysts are partial poisoning of the interior pore surface and pore-mouth plugging by deposition of metals from organo-metallic compounds in the reactor feed. A model is developed to account for both causes of deactivation. It can be used to predict which occurs first: complete surface poisoning or pore-mouth plugging. Equations are formulated for catalyst activity as a function of time for demetallization and also for desulfurization. The results depend upon particle geometry and geometry of deposited species, Thiele moduli for demetallization and desulfurization, and relative rates of desulfurization on fresh and partially poisoned catalytic surfaces. The treatment is for a single, isothermal catalyst particle.

BUM-JONG AHN and J. M. SMITH

University of California
Davis, CA 95616

SCOPE

The irreversible deposition of metals, particularly vanadium and nickel, has been identified as a major cause of deactivation of hydrodesulfurization (HDS) catalysts. Tamm et al. (1981) has presented experimental data suggesting that partial surface poisoning by metals deposition is responsible for the initial rapid deactivation while pore-mouth plugging is predominant at longer times. Deactivation by pore plugging has been carefully analyzed mathematically by Rajagoplan and Luss (1979). They included the effect of restricted diffusivities in the pore when the metal deposit reduces the pore radius to the same magnitude as the size of the organo-metallic molecules.

A similar quantitative treatment of the effects of combined partial surface poisoning and pore-mouth plugging on HDS catalyst activity does not appear to have been published. Our objective is to present such a combined model, which, amongst other aspects, will describe the conditions for which pore plugging will occur prior to complete surface poisoning. Since the large organo-metallic molecules have low diffusivities, the shell model of deactivation (Masamune and Smith, 1966) is employed to treat partial surface poisoning. The mathematical development is restricted to isothermal behavior of a single catalyst pellet with uniform pore-size distribution. First-order demetallization and desulfurization kinetics are assumed.

CONCLUSIONS AND SIGNIFICANCE

The deactivation by metals deposition on HDS catalysts, due to the combination of partial surface poisoning and pore-mouth plugging, is described quantitatively in terms of two parameters. These are the Thiele modulus φ_m for metals deposition and a partial poisoning parameter τ which depends, among other quantities, on the porosity of the catalyst and the density of the metal deposits. For large values of φ_m and τ, it is shown that the pore mouth is physically blocked before the deposited metal reaches the center of the catalyst particle. When this occurs demetallization and HDS activity are reduced to zero even though only partially poisoned and fresh catalyst surface still exist within the particle. For small values of φ_m and τ all the pore surface becomes partially deactivated before pore plugging occurs. Then some demetallization and HDS activity are retained.

From these concepts the ratio of demetallization activity at any time to that with a monolayer metal deposit has been evaluated as a function of φ_m and τ. By introducing two additional parameters, the Thiele modulus φ_s for desulfurization and the ratio b of the rate constants for HDS on the fresh and partially poisoned surface, HDS activity has also been calculated as a function of on-stream time. The results show that for constant φ_s, larger values of φ_m reduce the demetallization activity but increase the desulfurization activity. This is a consequence of the relative large intraparticle diffusion resistance for demetallization. The value of τ, which is defined as the ratio of the time required for complete surface poisoning to that for filling the pore with deposited metal species, affects HDS activity more than demetallization activity, particularly when φ_m is large.

Application of the model for the prediction of the temperature vs. time relationship for constant desulfurization activity is discussed. Increasing temperature over the life of the catalyst bed, in order to achieve a prescribed extent of desulfurization, is the operating procedure used in practice.

The proposed model should be of interest for establishing catalyst properties (including pore size distribution) which give optimum activity and life, although this has not been considered here.

As refining of heavy crudes and residual oils has become more widespread, hydrodesulfurization (HDS) processes have become more important. Heavy feed stocks often contain metal atoms, present in asphaltene and resin-type molecules, in concentrations of the order of 100 ppm (Douwes, et al., 1979). These metals, particularly nickel and vanadium, deposit on the catalyst lowering their desulfurization activity. Hence, reducing sulfur in heavy oils is more difficult than it is with light distillates. The metal-containing asphaltenes have been described (Yen et al., 1961) as consisting of layers of condensed aromatic rings with aliphatic side chains. Molecular size seems to be spread around an average of 100 Å or less but varies with the crude source (Richardson and Alley,

1975). Because of the large molecular size, metal deposition rates are severely retarded by diffusion in the pores of the HDS catalyst.

Desulfurization is usually carried out in trickle-bed reactors (cocurrent flow of hydrogen and liquid oil downward over a fixed bed of catalyst particles) where the sulfur containing molecule is converted to a hydrocarbon with the production of hydrogen sulfide. In practice constant desulfurization is sought by increasing the reactor temperature over the life of the catalyst. Such lifetimes normally range from months to years, depending primarily on the metals content of the oil feed, the catalyst, and the required degree of desulfurization. Short lifetimes and the difficulty of regeneration have become major economic factors in desulfurization processing.

The usual cobalt-molybdenum catalyst on a silica-alumina carrier has a significant volume of small pores (and accompanying relatively large surface area) so that intraparticle diffusion affects global kinetics. Deactivation is caused by metals and coke deposition, but the former largely determines catalyst life. From extensive pilot-plant data Tamm et al. (1981) have shown that the normal temperature vs. time curve consists of three parts: an initial period when the temperature must be increased rapidly to obtain constant extent of desulfurization, a longer intermediate period when the temperature may be increased slowly, and a final period of rapid increase. These results were interpreted in terms of activity as: 1) an initial period of rapid loss in activity; 2) a relatively long period during which there is a slower continuous drop in activity; and 3) at longer times another rapid decrease in activity. The first stage has been attributed in part to coke deposition, but Tamm et al. (1981) have suggested that metals deposition, with accompanying partial poisoning of the covered sites (the deposited metals themselves have some desulfurization activity), is the cause. Evidence for this conclusion is that the time period for this initial loss in activity was found to be directly related to the concentration of organometallics in the feed rather than proportional to the residual carbon content (coke precursors). During the second-stage multilayer, metal deposition occurs. Since metal deposition is strongly limited by diffusion (Fazli-Khosrochahi and Kieffer, 1975; Sato et al., 1971; Tamm et al., 1981), the metals buildup will be most severe at the pore mouth. Hence, during this second stage it is postulated that pore-mouth plugging occurs, first in the smaller pores and then continuing in the larger pores. In the last stage, most of the bed has become inactive due to pore plugging and the temperature must be increased to a very high value in order to achieve the desired extent of desulfurization.

Several models have been used to predict catalyst life. For example, Newson (1975) considered how pore plugging alone affects catalyst activity. The thickness of the metal deposit was assumed to be uniform over a fraction of the pore length measured from the outer surface of the catalyst particle. Dautzenberg et al. (1978) proposed a more complex model to allow for variation of the thickness of the metal deposit (on the pore wall) with time and radial position in the particle. Deactivation was assumed to be due to the decrease with time of the cross-sectional area of the pore mouth.

Hughes and Mann (1978) postulated a wedge-shaped metals deposit so that the maximum thickness of the wedge determined when pore-plugging occurred, while the length of the wedge, corresponding to the penetration of the deposit into the particle, determined the extent of partial surface poisoning.

Rajagoplan and Luss (1979) developed a mathematical model to explain the effect of pore plugging. They accounted quantitatively for the variation in diffusivity of the large organometallic compounds with the pore diameter by using the relationship suggested by Spry and Sawyer (1975). In trickle-bed reactors the pores are probably filled with liquid, but in small pores the diffusivity is less than the conventional molecular value due to steric hindrance and enhanced drag at the pore wall. We will use the same Spry and Sawyer relationship in this paper.

The prior models have not accounted quantitatively for both partial surface poisoning that occurs at short times and pore plugging. The shell model employed by Masamune and Smith (1966) can be used to describe partial surface poisoning since the diffusion resistance is large for the metal deposition. We will use this shell concept, which assumes that there is a sharp boundary separating the partially deactivated outer shell and the inner core of fresh catalyst. The objective is to develop a composite model which will account, by metal deposition, for both partial surface poisoning at short times and pore plugging at longer times. Coke formation and its effect on catalyst activity are neglected. The development is based upon isothermal reactions in a single particle, but reduction in pore diameter with time and radial position within the particle is included.

Published kinetics studies (Dautzenberg et al., 1978; Beuther and Schmid, 1963; Chang and Silvestri, 1974; Gates et al., 1979; Satterfield and Roberts, 1968; Speight, 1981; Shah and Paraskos, 1975) have correlated experimental data for both hydrodemetallization and hydrodesulfurization by first and second order and Langmuir-Hindshelwood rate equations. In the concentration range where the hydrogen concentration in the liquid is much greater than the contaminant concentration, pseudofirst-order kinetics appears to be applicable. In the following treatment a first-order rate expression is used for both demetallization and desulfurization.

MODEL OF CATALYST DEACTIVATION IN A SINGLE PARTICLE

Consider a single pore in the catalyst particle. It is assumed that the rate of metal deposition on fresh catalyst is controlled by intraparticle diffusion. Metal deposition also occurs on the deposited metal surface but at a slower rate, governed by a rate constant k_m. Then the thickness of the deposited metal layer will grow with time at any intraparticle position. This thickness will be greatest at the pore mouth and, for an intermediate time, decrease to monomolecular layer at a radial position r_i. This situation is shown schematically in Figure 1a. Since the rate of metal deposition is very fast with respect to the rate of diffusion, a sharp boundary, separating fresh and fouled catalyst exists at r_i. The monolayer thickness at r_i is just sufficient to reduce the rate constant for further metal deposition to k_m.

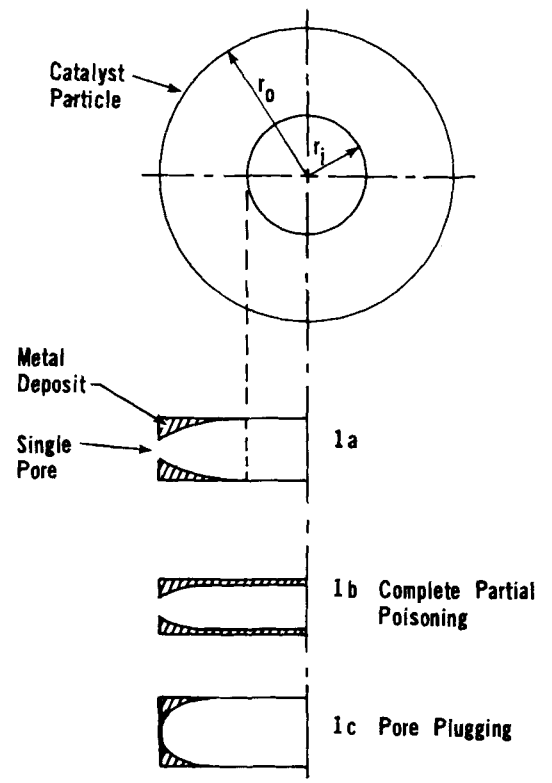

Figure 1. Model for partial surface poisoning and pore plugging.

Simultaneous with demetallization, desulfurization reactions occur, both in the partially fouled shell and fresh inner core of catalyst, but at different rates according to rate constants k_s and bk_s, respectively.

The results of Masamune and Smith (1966) indicate that the shell model, just described, predicts slightly faster deactivation than the more general solution. The latter allows for a variation in fraction of fouled surface with radial position in the particle. Hence some reaction occurs in the general solution in outer sections of the catalyst particle where the reactant concentration is higher.

As time proceeds, metal deposition will lead to one of two end results, depending in part upon pore size and rates of demetallization. For relatively large pores and a *relatively* slow rate, r_i will become zero so that the entire pore contains metal deposits but the pore mouth remains open. Such a pore, shown in Figure 1b, still is active for both demetallization and desulfurization but at reduced rates. For small pores and a more rapid demetallization rate, the metal deposit will build up rapidly near the outer surface of the particle (r_i is large). Soon the mouth of the pore will become plugged and both demetallization and desulfurization will cease. In this case, shown in Figure 1c, the lifetime of the pore will be shorter but its activity higher than for the pore of Figure 1b. In a catalyst particle with a distribution of pore sizes both cases could occur simultaneously in different pores.

DEMETALLIZATION

There is evidence (Anderson and Quinn, 1974; Spry and Sawyer, 1975) that the diffusivity of the large organo-metallic compounds is hindered in small pores. Thus, the conventional expression for the effective diffusivity in terms of a tortuosity factor τ_p and porosity ϵ, may be modified to the form

$$D_m = \frac{\epsilon D_\infty}{\tau_p} G(\lambda) \tag{1}$$

where λ is the ratio of the size of the organo-metallic molecule to the pore radius, that is r_m/r_p. In the absence of more fundamental information about $G(\lambda)$ we will use the empirical relation

$$G(\lambda) = (1 - \lambda)^4 \tag{2}$$

proposed by Spry and Sawyer (1975). Another approach would be to employ the statistical procedure of Morrison (1965). Satterfield et al. (1973) suggested an exponential dependence of D_m on r_m/r_p which is not much different than Eq. 2; Rajagoplan and Luss (1979) employed Eq. 2 in their treatment of pore plugging. The effective diffusivity in the partially poisoned shell ($r_i < r < r_o$) will vary with time, because r_p varies with time, and also vary with r. In applying the shell model pseudo-steady state is assumed. This last restriction should be satisfactory since the change in r_i with time will be slower than the diffusion rate in the liquid-filled pores. However, the assumption is not as valid as it is for a gaseous reactant. This is because the density difference between the diffusing reactant, when it is a liquid, and the deposited metal species is not as great as when the diffusing reactant is a gas.

Equations for Partially Poisoned Pores ($r_i < r_o$)

The mass conservation equation for the organo-metallic reactant in the shell ($r_i \le r \le r_o$) may be written as

$$\frac{1}{r^2}\frac{d}{dr}\left[r^2\left(\frac{r_p}{r_{p_o}}\right)^2 D_m \frac{dC_m}{dr}\right] - \rho k_m \left(\frac{r_p}{r_{p_o}}\right) C_m = 0 \tag{3}$$

with boundary conditions

$$C_m = C_{m_o} \text{ at } r = r_o \tag{4}$$

$$C_m = 0 \text{ at } r = r_i \tag{5}$$

The factor (r_p/r_{p_o}) appears in the reaction term of Eq. 3 because it is supposed that the rate is proportional to the surface. Thus, the constant k_m must be multiplied by r_p/r_{p_o} to account for the change in surface area of the cylindrical pore as metals are deposited. Boundary condition 5 requires that either the metals deposition reaction is severely diffusion limited, or that the poisoning reaction in the fresh core is much faster than that on the metal containing surface. As mentioned earlier there is evidence that the first requirement is likely to be valid. Boundary condition 5 cannot be exactly true when r_i approaches zero or r_o. However, numerical calculations with Eq. 5 and with the symmetric condition at $r = 0$, $dC_m/dr = 0$, show little difference; Eq. 5 predicts a slightly faster deactivation rate, which is conservative. When the pore is completely covered with a metal deposit but the pore mouth not yet closed ($r_p > r_m$), the symmetric condition is employed.

The equation relating the rate of change of the boundary at r_i with time and the open-pore radius r_p is

$$-\pi \frac{\rho q_o}{\alpha} r_i^2 \left(\frac{dr_i}{dt}\right) = r_o^2 \left(D_m \frac{dC_m}{dr}\right)_{r=r_o} - \int_{r_i}^{r_o} \rho k_m \left(\frac{r_p}{r_{p_o}}\right) r^2 C_m dr \tag{6}$$

with initial condition

$$r_i = r_o \text{ at } t = 0 \tag{7}$$

The rate of change of open-pore radius due to metal deposition is also a function of r and t, and is given by the equation

$$-(2\pi r_p) n l \rho_m \frac{dr_p}{dt} = \alpha M_p \frac{r_p}{r_{p_o}} k_m C_m \tag{8}$$

subject to the initial condition

$$r_p = r_{p_o} \text{ at } t = 0 \tag{9}$$

The unknown pore length l and the number n of pores of length l per unit mass of catalyst are related to the particle porosity and density by

$$n l \pi r_{p_o}^2 = \epsilon/\rho \tag{10}$$

The three equations (Eqs. 3, 6 and 8) can be solved simultaneously for r_p and r_i as a function of time. Particular solutions can be obtained for t when $r_i = 0$ and when $r_p = r_m$. These results show whether complete partial poisoning ($r_i = 0$) or pore-plugging ($r_p = r_m$) occurs first.

In dimensionless form Eqs. 3–9 become

$$\frac{1}{\xi^2}\frac{d}{d\xi}\left(\xi^2 g \frac{d\overline{X}_m}{d\xi}\right) - \phi_m^2 \xi_p \overline{X}_m = 0 \tag{11}$$

$$\overline{X}_m = 1 \text{ for } \xi = 1 \tag{12}$$

$$\overline{X}_m = 0 \text{ for } \xi = \xi_i \tag{13}$$

$$-\xi_i^2 \frac{d\xi_i}{d\theta} = \frac{1}{\tau}\left[\frac{1}{\phi_m^2}\left(g\frac{d\overline{X}_m}{d\xi}\right)_{\xi=1} - \int_{\xi_i}^{1} \xi_p \xi^2 \overline{X}_m d\xi\right] \tag{14}$$

$$\xi_i = 1 \text{ at } \theta = 0 \tag{15}$$

$$\frac{d\xi_p}{d\theta} = -\overline{X}_m \tag{16}$$

$$\xi_p = 1 \text{ at } \theta = 0 \tag{17}$$

where the dimensionless variables are

$$\xi = r/r_o \tag{18}$$

$$\xi_i = r_i/r_o \tag{19}$$

$$\xi_p = r_p/r_{p_o} \tag{20}$$

$$\overline{X}_m = C_m/C_{m_o} \tag{21}$$

$$g = (r_p/r_{p_o})^2(1 - r_m/r_p)^4/(1 - r_m/r_{p_o})^4 \tag{22}$$

$$\theta = t/t_f \tag{23}$$

and the parameters are defined as follows:

$$\phi_m = r_o \left(\frac{\rho k_m}{D_{m_o}}\right)^{1/2} \tag{24}$$

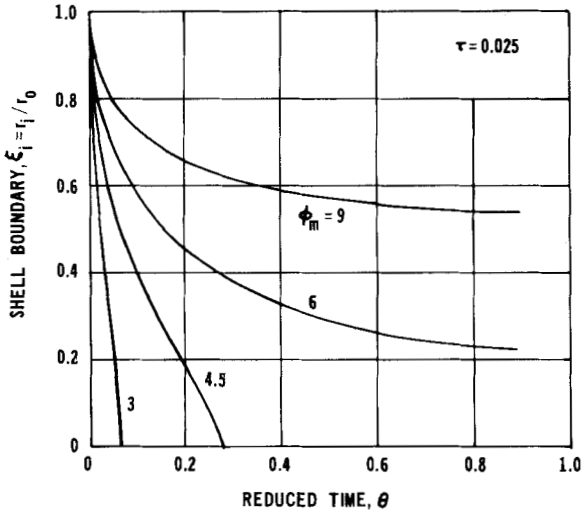

Figure 2. Change of shell boundary with time due to demetallization (τ = 0.025).

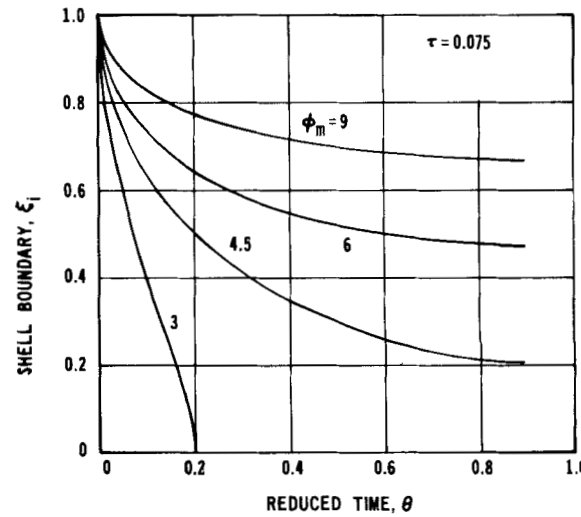

Figure 4. Shell boundary change with time due to demetallization (τ = 0.075).

$$\tau = \frac{q_o M_p \rho}{2\rho_m \epsilon} = t_s/t_f \tag{25}$$

where

$$t_f = \frac{2\epsilon\rho_m}{\alpha\rho M_p k_m (C_{m_o})} \tag{26}$$

and

$$t_s = q_o/\alpha k_m C_{m_o} \tag{26a}$$

Dimensionless Equations (Eqs. 11–17) describe a demetallization model with two parameters, the Thiele modulus ϕ_m and a dimensionless time-constant τ for partial surface poisoning.

Equations 11, 14 and 16 were solved numerically for the location ξ_i of the shell boundary as a function of time and for the profiles of metal deposit thickness, ξ_p and concentration $\overline{X}_m$ as a function of reduced time θ and position ξ. Pseudosteady-state Equation (Eq. 11) was solved first using a finite difference scheme with 75 to 150 nodal points, depending on the value of r_i. The metal concentration $\overline{X}_m$ was then employed to obtain revised values of the diffusivity g from Eq. 22, ξ_i from Eq. 14, and ξ_p from Eq. 16. The results were substituted back into Eq. 11. The computations were continued until the shell boundary reaches the center of the particle or the pore mouth becomes plugged. In solving Eq. 14, the two terms on the right side were evaluated in the domain between $(1 + \xi_i)/2$ and ξ_i in order to avoid difficulties in numerical differentiation to obtain the gradient $d\overline{X}_m/d\xi$ at $\xi = 1$. At short times, θ was calculated for a chosen inward progression of the boundary ξ_i.

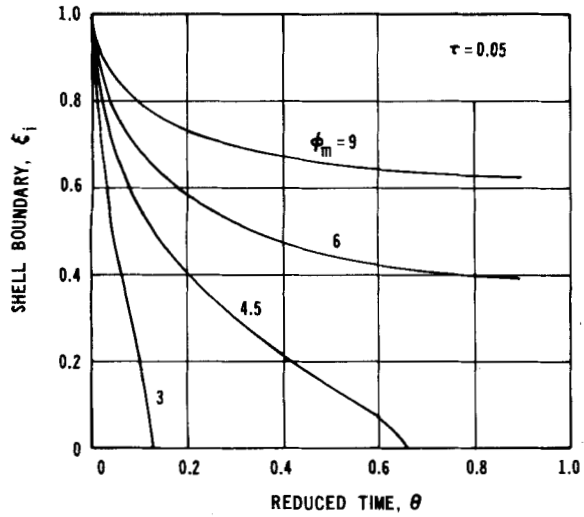

Figure 3. Shell boundary change with time due to demetallization (τ = 0.05).

Results for Partially Poisoned Pores

Figures 2, 3, and 4 show how the shell boundary r_i varies with reduced time in plots of ξ_i *vs.* θ. Figure 2 displays the effect of the Thiele modulus ϕ_m for a constant value of the constant (τ) of 0.025. Figures 3 and 4 are for τ = 0.05 and 0.075, respectively. These figures illustrate the effect of the two parameters on complete partial poisoning and pore plugging. For example, in Figure 2 the curves for ϕ_m = 3 and 4.5 show that r_i becomes zero before (at lower values of θ) pore plugging occurs. Pore plugging is assumed when the pore radius r_p is equal to the size of the organometallic molecule. Figures 2–4 are for a molecule size of 0.1 of the initial pore radius, that is, $r_m = 0.1\ r_{p_o}$. Integrating Eq. 16 at the pore mouth where $\overline{X}_m = C_m/C_{m_o} = 1$, there is obtained

$$\xi_p = \frac{r_p}{r_{p_o}} = 1 - \theta \tag{27}$$

For $r_p = r_m = 0.1\ r_{p_o}$, Eq. 27 gives $\theta = 0.9$. Hence, $r_m/r_{p_o} = 0.1$ is equivalent to a reduced time, θ, of 0.9. Since $r_i = 0$ for curves of ϕ_m = 3 and 4.5 (Figure 2) at θ values less than 0.9, complete partial poisoning occurs prior to pore plugging. For these conditions the catalyst still has some demetallization (and desulfurization) activity beyond the time for which $r_i = 0$. In contrast, the curves for ϕ_m = 6 or 9 in Figure 2 reach $\theta = 0.9$ before $\xi_i = 0$ (or $r_i = 0$). Hence pore plugging and complete loss in catalyst activity occurs prior to complete partial poisoning. This is also evident from the fact that

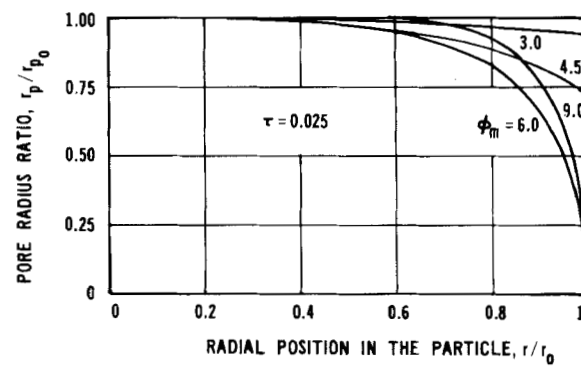

Figure 5. Metal deposit profiles (for r_m/r_{p_o} = 0.1).

the curves become horizontal (no further change in r_i with time) at finite values of ξ_i. Analogous results could be obtained for any choice of the value of r_m.

Comparison of the curves in Figure 2–4 for the same ϕ_m (for example, $\phi_m = 4.5$) shows that the value of τ has a strong influence on the time for complete surface poisoning and whether or not this time is less than that for pore plugging. Equation 25 shows that the value of τ depends upon the catalyst porosity and density and the chemical and physical properties q_o, M_p, ρ_m; τ can be considered a surface poisoning parameter, equal to the ratio, t_s/t_f. The time t_s is the time that would be required to cover the entire pore surface with the minimum concentration q_o. The time t_f is that corresponding to the amount of metal deposition necessary to fill the entire pore volume with metal deposit.

Figure 5 shows the decrease in pore radius, plotted as r_p/r_{p_o}, with increasing distance along the pore toward the pore mouth. The figure is for $\tau = 0.025$, corresponding to Figure 2. The curves for $\phi_m = 3.0$ and 4.5 show again that complete surface poisoning occurs prior to pore plugging, $r_p/r_{p_o} > 0.1$, at the pore mouth ($r/r_o = 1.0$). For $\phi_m = 6.0$ and 9.0 pore plugging occurs ($r_p/r_{p_o} = 0.1$) at the pore mouth.

Complete Surface Poisoning ($r_f = 0$)

After r_i becomes zero, further catalyst deactivation will result solely from the decrease in pore radius, and accompanying decrease in diffusivity due to metals deposition. For this situation Eqs. 3 and 8 are still applicable (Eq. 6 is no longer involved), but the boundary condition given by Eq. 5 is replaced by

$$\frac{dC_m}{dr} = 0 \text{ at } r = 0$$

or

$$\frac{d\bar{X}_m}{d\xi} = 0 \text{ at } \xi = 0 \tag{28}$$

Equations 11, 12, 28, 16 and 17 describe deactivation after $r_i = 0$ for the remaining life of the catalyst particle. During this period demetallization occurs throughout the pore at a reduced rate (with respect to fresh catalyst) determined by rate constant k_m and the concentration C_m along the pore. This concentration is reduced since the diffusivity decreases as a result of the decrease in r_p. This decrease in D_m is most severe at the pore mouth because the metals deposit will be greatest at this location. Equations 11, 12, 28, 16 and 17 are solved numerically for the profile of metal deposit thickness ξ_p and concentration profile $\bar{X}_m$ as a function of θ and ξ.

Deactivation Results for All r_f

The rate of demetallization for all r_i can be conveniently represented by an activity ratio, or effectiveness factor $\eta_m(t)$. This ratio is the rate of organo-metallic entering the pore to the rate if there were no intraparticle diffusion resistance so that demetallization was determined by k_m and C_{m_o}. In equation form

$$\eta_m(t) = \frac{\left\{r_o^2\left(\frac{r_p}{r_{p_o}}\right)^2 D_m\left(\frac{dC_m}{dr}\right)\right\}_{r=r_o}}{\left(\frac{1}{3}\right) r_o^3 \rho k_m C_{m_o}} \tag{29}$$

or

$$\eta_m(t) = \frac{\int_{r_i}^{r_o} r^2 \rho k_m \frac{r_p}{r_{p_o}} C_m dr + \left[r^2\left(\frac{r_p}{r_{p_o}}\right)^2 D_m \frac{dC_m}{dr}\right]_{r=(r_o+r_i)/2} - \int_{r_i}^{(r_o+r_i)/2} \rho r^2 k_m \left(\frac{r_p}{r_{p_o}}\right) C_m dr}{\frac{1}{3}(r_o^3 \rho k_m C_{m_o})} \tag{30}$$

With dimensionless quantities this last equation becomes

$$\eta_m(\theta) = 3\int_{\xi_i}^{1} \xi^2 \xi_p \bar{X}_m d\xi + 3\left[\frac{1}{\phi_m^2}\left(\xi_g^2 \frac{d\bar{X}_m}{d\xi}\right)_{\xi=(1+\xi_i)/2} - \int_{\xi_i}^{(1+\xi_i)/2} \xi^2 \xi_p \bar{X}_m d\xi\right] \tag{31}$$

Figures 6 and 7 show the activity for demetallization calculated from Eq. 31 for various Thiele moduli and surface-poisoning parameter (τ) values. Comparison of the two figures indicates that

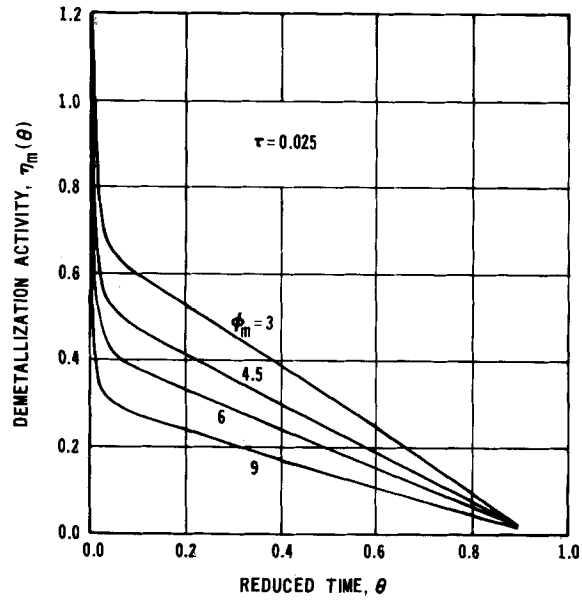

Figure 6. Demetallization activity as a function of time ($\tau = 0.025$).

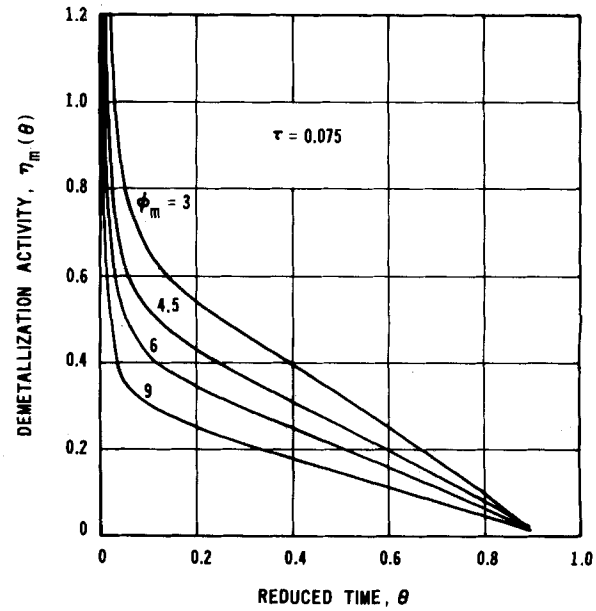

Figure 7. Demetallization activity as a function of time ($\tau = 0.075$).

τ has a significant effect on activity at short times where surface poisoning is predominant. Thus, when τ is large (Figure 7), for example, due to a larger q_o required for surface poisoning, the activity at a given time is larger than that for a low τ (Figure 6). At long times where pore plugging is dominant τ has little effect. In contrast ϕ_m, which reflects diffusion resistance, has a large effect over the complete range of θ. Values of the activity can be greater than unity since for $r_i > 0$, the demetallization rate can be higher than that in the denominator in Eq. 29 which is based upon complete surface poisoning ($r_i = 0$).

DESULFURIZATION

If the sulfur-containing molecules are smaller than those with metal atoms, the effective diffusivity D_s is expected to be larger than D_m. Provided D_s is much greater than D_m, as suggested by Newson (1975), the Thiele modulus ϕ_s for desulfurization would be independent of the extent of metals deposition and, therefore, would be constant with respect to time and position along the pore. In the quantitative treatment that follows this assumption will be made. Then the activity for desulfurization will decrease with time because the rate constant k_s on surface covered by metals is less than bk_s on the fresh surface, and because metals deposition reduces the catalytic surface by decreasing the pore radius.

According to the foregoing concepts, the mass balance for the sulfur-containing molecules of concentration C_s in the poisoned shell ($r_i \le r \le r_o$) may be written

$$\frac{D_s}{r^2}\frac{d}{dr}\left[r^2\left(\frac{r_p}{r_{p_o}}\right)^2\frac{dC_s}{dr}\right] - \rho k_s\left(\frac{r_p}{r_{p_o}}\right)C_s = 0 \tag{32}$$

For the fresh catalyst in the core ($0 \le r \le r_i$) the mass balance is

$$\frac{D_s}{r^2}\frac{d}{dr}\left(r^2\frac{dC_s}{dr}\right) - \rho(bk_s)C_s = 0 \tag{33}$$

The boundary conditions are

$$C_s = C_{s_o} \text{ at } r = r_o \tag{34}$$

$$C_{s,r_i+0} = C_{s,r_i-0} \text{ at } r = r_i \tag{35}$$

$$\left(\frac{dC_s}{dr}\right)_{r_i+0} = \left(\frac{dC_s}{dr}\right)_{r_i-0} \text{ at } r = r_i \tag{36}$$

$$\frac{dC_s}{dr} = 0 \text{ at } r = 0 \tag{37}$$

In dimensionless form, with

$$\phi_s = r_o\left(\frac{\rho k_s}{D_{s_o}}\right)^{1/2}; \quad \overline{X}_s = C_s/C_{s_o} \tag{38}$$

Equations 32–37 become

$$\frac{1}{\xi^2}\frac{d}{d\xi}\left(\xi^2\xi_p^2\frac{d\overline{X}_s}{d\xi}\right) - \phi_s^2\xi_p\overline{X}_s = 0; \quad \xi_i \le \xi \le 1 \tag{39}$$

$$\frac{1}{\xi^2}\frac{d}{d\xi}\left(\xi^2\frac{d\overline{X}_s}{d\xi}\right) - \phi_s^2 b\overline{X}_s = 0; \quad 0 \le \xi \le \xi_i \tag{40}$$

$$\overline{X}_s = 1, \text{ at } \xi = 1 \tag{41}$$

$$\overline{X}_{s,\xi_i+0} = \overline{X}_{s,\xi_i-0}, \text{ at } \xi = \xi_i \tag{42}$$

$$\left(\frac{d\overline{X}_s}{d\xi}\right)_{\xi_i+0} = \left(\frac{d\overline{X}_s}{d\xi}\right)_{\xi_i-0}, \text{ at } \xi = \xi_i \tag{43}$$

$$\frac{d\overline{X}_s}{d\xi} = 0 \text{ at } \xi = 0 \tag{44}$$

Equations 39–44 can be solved for the concentration profile of sulfur species, $\overline{X}_s$ vs. ξ, (or C_s vs. r) at any time. In carrying out the solution, metal deposition (Eqs. 11, 14 and 16 or 11, 16) is solved simultaneously to find out how the pore radius varies with position ξ along the pore and with time θ. Once the sulfur concentration profile has been determined, the activity ratio $\eta_s(t)$ for desulfurization can be calculated from the following equation:

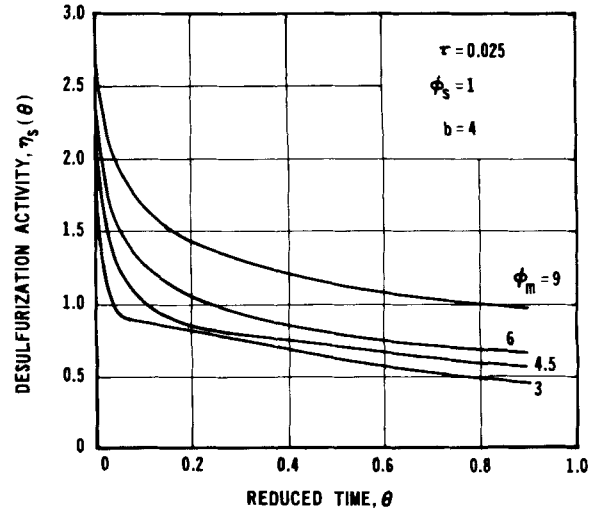

Figure 8. Desulfurization activity as a function of time (τ = 0.025).

$$\eta_s(t) = \frac{\displaystyle\int_0^{r_i} r^2\rho(bk_s)C_s dr + \int_{r_i}^{r_o}\rho r^2 k_s\left(\frac{r_p}{r_{p_o}}\right)C_s dr}{\left(\frac{1}{3}\right)r_o^3\rho k_s C_{s_o}} \tag{45}$$

which in dimensionless form becomes

$$\eta_s(\theta) = 3\left\{b\int_0^{\xi_i}\xi^2\overline{X}_s d\xi + \int_{\xi_i}^{1}\xi^2\xi_p\overline{X}_s d\xi\right\} \tag{46}$$

Equation 45 shows how the HDS activity of the catalyst varies with time. The normalization in Eq. 45 is with respect to complete partial poisoning, that is, with respect to a reaction rate based upon metal-covered surface. Hence, $\eta_s(t)$ can have values greater than unity. This will occur when the metal-covered shell is thin (r_i only a little less than r_o) so that most of the desulfurization takes place in the core of fresh catalyst for which the rate constant is bk_s.

Equation 45 or 46 is applicable when $0 < r_i < r_o$. After r_i becomes zero further desulfurization occurs only on metal-covered surface. Then Eqs. 39, 41 and 44 determine the sulfur concentration profile in the pore. The activity ratio, or effectiveness factor, is calculated from the expression

$$\eta_s(\theta) = 3\int_0^1 \xi^2\xi_p\overline{X}_s d\xi \tag{47}$$

Figures 8 and 9 display the desulfurization activity ratio vs. reduced time for the same values of the time constant (τ) for partial surface poisoning as used in Figures 6 and 7. The results shown are

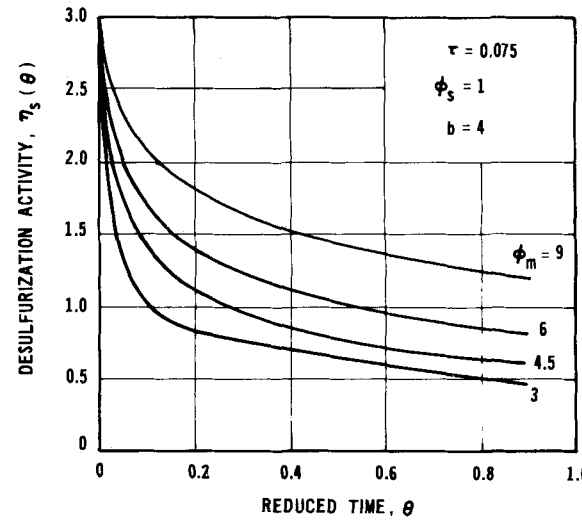

Figure 9. Desulfurization activity as a function of time (τ = 0.075).

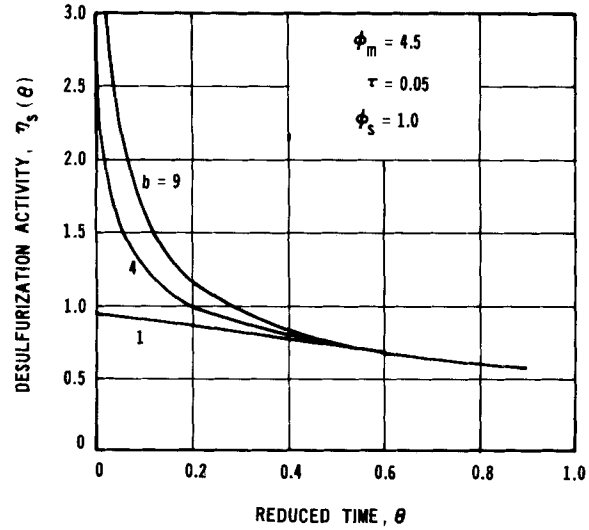

Figure 10. Effect of rate-constant ratio b on desulfurization activity (complete surface poisoning prior to pore plugging).

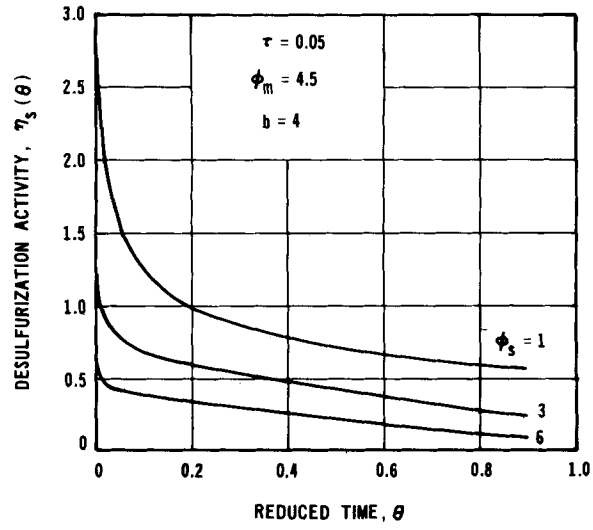

Figure 12. Effect of Thiele Modulus ϕ_s on desulfurization activity (complete surface poisoning prior to pore plugging).

for $\phi_s = 1$ and $b = 4$, corresponding to a relatively small amount of intraparticle diffusion resistance for the sulfur-containing molecules and a desulfurization rate on the metal-covered surface one fourth of the rate on the fresh surface. The curves in Figures 8 and 9 are of the same general form as those in Figures 6 and 7. Both show a sharp drop in activity at low times followed by a nearly linear fall at higher θ where r_i has reached zero, corresponding to complete surface poisoning.

The drop in activity for metals deposition (Figures 6 and 7) is steeper than that for desulfurization (Figures 8 and 9) because of the shell model assumption for demetallization. That is, the demetallization rate constant on the fresh catalyst is very large with respect to that (k_m) on the partially poisoned surface. In contrast, the two desulfurization rate constants employed for Figures 8 and 9 differ but fourfold. The effect of the ratio, b, of rate constants on the curves for desulfurization activity is shown in Figure 10. These curves are for the case of complete surface poisoning preceding pore-mouth plugging; that is, r_i becomes zero before $r_p = r_m$. For $b = 9$ the fall in activity is steeper than for $b = 1$ or 4, and the shape of the curve approaches more closely that for demetallization. Note that the activities become independent of b at long times. Deactivation at these times, when all the surface has been covered with metals, depends on the rate constant k_s and not on bk_s.

Figure 11 illustrates, for chosen values of ϕ_m, ϕ_s and τ, activity

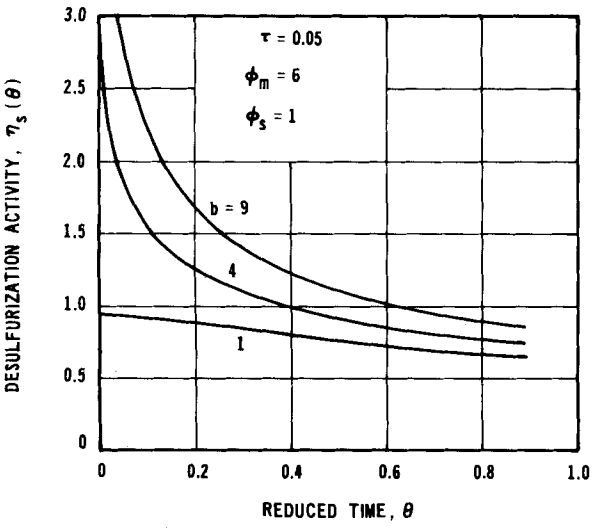

Figure 11. Effect of rate-constant ratio b on desulfurization activity (pore plugging prior to complete surface poisoning).

curves when pore-mouth plugging occurs before complete surface poisoning (before r_i becomes zero). Comparison of Figures 10 and 11 suggests that when pore plugging occurs first, the catalyst may have a higher activity over the entire lifetime than a catalyst for which complete surface poisoning occurs first. Figure 11 is for $\phi_m = 6$, while in Figure 10 $\phi_m = 4.5$ because a higher value is necessary in order that pore plugging occurs first. Thus Figure 3 shows that pore plugging occurs first for $\phi_m = 6$ while for $\phi_m = 4.5$ complete surface poisoning occurs first.

Figure 12 describes the effect of the Thiele modulus for desulfurization on the decay in activity. The curves are for the case where complete surface poisoning occurs prior to pore plugging and are analogous to those in Figure 10. As ϕ_s increases from 1 to 6, Figure 12 shows that the initial drop in activity becomes much greater. When ϕ_s is large the desulfurization reaction occurs predominantly in the outer shell of the catalyst. This is precisely the region where the metals are deposited first and, therefore, where the rate of desulfurization is the lowest. The values of ϕ_s and ϕ_m shown in Figures 8 to 12 were estimated from expected values of the parameters.

Temperature vs. Time Curves

As mentioned, HDS plants are normally operated by increasing the temperature over the lifetime of the catalyst in order to maintain constant extent of desulfurization. It is of interest to discuss how the constant-temperature single-particle model presented here might be used to predict temperature vs. time, constant activity, and curves. The calculational procedure is straightforward for a particular location in the reactor. The local rate of reaction may be written

$$\text{Rate} = \frac{4}{3}\pi r_o^3 C_{s_o}[\eta_s(t)k_s] \tag{48}$$

where $\eta_s(t)$ is given by Eq. 45 or 47. In Eq. 48 the product $[\eta_s(t)]k_s$ determines how the rate or activity varies with time. Curves similar to those in Figures 8, 9 or 12 could be prepared for a range of values of the parameters ϕ_m, ϕ_s and b. To relate these results to temperature, the dependence of k_m, k_s and b, and diffusivities D_m and D_s on T would be necessary. Next, curves of $\eta_s(t)k_s$ vs. t would be made. Then for various times the values of ϕ_s at constant $[\eta_s(t)k_s]$ could be determined. Finally, the temperature associated with ϕ_s would be noted from the data for the dependence of k_s and D_s on temperature. If interphase (particle-fluid) mass transfer retarded the rate, interphase boundary conditions would be required to relate C_s to the bulk fluid concentration of the sulfur-containing compound.

For an integral reactor, the procedure is more complex. Intrareactor mass conservation equations would need to be integrated after solving demetallization and desulfurization intraparticle expressions, Eqs. 3, 6, 8, 32 and 33. Again interphase boundary conditions might be required in order to obtain the sulfur species concentration in the bulk fluid phase. By this procedure sulfur concentrations in the reactor effluent could be calculated as a function of the several intraparticle, interphase and intrareactor parameters. Such results could be used to predict the temperature vs. time curves required for a constant fractional conversion of sulfur in the reactor feed.

ACKNOWLEDGMENT

The financial assistance of NSF Grant CPE-8026101 is gratefully acknowledged. We also would like to thank Edward Sughrue and John Myers of Phillips Petroleum Co. for their helpful discussions.

NOTATION

b = ratio of desulfurization rate constant of the fresh core to that of the fouled shell
C_m = concentration of organo-metallic compounds in the liquid in the pores, mol/m^3; C_{m_o} = concentration at particle surface
C_s = concentration of sulfur-containing molecules in the liquid in the pores, mol/m^3; C_{s_o} = concentration at particle surface
D_m = effective diffusivity of the organo-metallic compounds, m^2/s; D_{m_o} = diffusivity at zero time
D_s = effective diffusivity of sulfur containing species, m^2/s; D_{s_o} = diffusivity at zero time
D_∞ = molecular diffusivity of the organo-metallic compounds, m^2/s
g = dimensionless effective diffusivity, defined by Eq. 22
k_m = rate constant for demetallization in the shell, m^3/kg·s
k_s = rate constant for desulfurization in the shell, m^3/kg·s
M_p = molecular weight of metal deposit, kg/kmol
n = number of pores with length l per unit mass of catalyst, kg^{-1}
q_o = concentration of deposited metals corresponding to a monolayer, kmol/kg
r = radial position in catalyst pellet, m
r_o = catalyst particle radius, m
r_t = radius of the boundary between fouled shell and fresh core of catalyst particle, m
r_p = pore radius, m
r_{p_o} = pore radius at time zero, m
r_m = radius of organo-metallic molecule, m
T = absolute temperature, K
t_s = time constant for complete surface poisoning, defined by Eq. 26a
t_f = time constant for metal deposit to fill entire pore volume, defined by Eq. 26, s
$\bar{X}_m$ = dimensionless concentration of organo-metallic compounds, C_m/C_{m_o}
$\bar{X}_s$ = dimensionless concentration of sulfur-containing molecules C_s/C_{s_o}

Greek Letters

α = number of deposited metal molecules per organo-metallic molecule
ϵ = porosity of catalyst particle
λ = ratio of size of metal-containing species to the pore radius, r_m/r_p
ρ = apparent density of catalyst particle, kg/m^3
ρ_m = density of metal deposit, kg/m^3
$\eta_m(t)$ = relative activity of demetallization, defined by Eq. 29
ϕ_m = Thiele modulus for demetallization defined by Eq. 24
$\eta_s(t)$ = relative activity of desulfurization, defined by Eq. 45
ϕ_s = Thiele modulus for desulfurization, defined by Eq. 38
ξ = dimensionless radial position in the pellet, r/r_o
ξ_t = dimensionless radius of the boundary, r_t/r_o
ξ_p = dimensionless pore radius, r_p/r_{p_o}
τ = ratio of time constants, t_s/t_f
τ_p = tortuosity of catalyst pellet
θ = dimensionless time, t/t_f

LITERATURE CITED

Anderson, J. L., and J. A. Quinn, "Restricted Transport in Small Pores; A Model for Steric Exclusion and Hindered Particle Motion," *Biophys. J.*, **14**, 130 (1974).

Beuther, H., and B. K. Schmid, "Reaction Mechanisms and Rates in Residue Hydrodesulfurization," Sixth World Petroleum Congress, Frankfurt, Proceedings, Sec. III, Paper 20-PD7, 297 (1963).

Chang, C. D., and A. J. Silvestri, "Manganese Nodules as Demetallation Catalysts," *Ind. Eng. Chem., Process Des. Dev.*, **13**, 315 (1974).

Dautenzenberg, F. M., et al., "Catalyst Deactivation through Pore Mouth Plugging during Residue Desulfurization," *ACS Symp. Ser.*, **65**, 254 (1978).

Douwes, C. T., et al., "Developments in Hydroconversion Processes of Residues," *Proc. of the Tenth World Petroleum Congress*, Bucharest, **4**, 175 (1979).

Fazli-Khosrochahi, R., and R. Kieffer, "Contribution à l'étude de l'hydrodésulfuration. III: Influence des caractéristiques du catalyseur, Mode d'action du poison," *Bull. Soc. Chim. France*, No. 3-4, 727 (1975).

Gates, B. C., J. R. Katzer, and G. C. A. Shuit, *Chemistry of Catalytic Processes*, McGraw-Hill, New York (1979).

Hughes, C. C., and R. Mann, "Interpretation of Catalyst Deactivation by Fouling from Interactions of Pore Structure and Foulant Deposit Geometrics," *ACS Symp. Ser.*, **65**, 201 (1978).

Masamune, S., and J. M. Smith, "Performance of Fouled Catalyst Pellets," *AIChE J.*, **12**(2), 384 (1966).

Morrison, M. E., "The Rate and Mechanism of the Air Oxidation of NO," Ph.D. Thesis, Proposition V, Calif. Inst. of Tech., Pasadena, CA (April, 1965).

Newson, E., "Catalyst Deactivation due to Pore-Plugging by Reaction Products," *Ind. Eng. Chem., Process Des. Dev.*, **14**(1), 27 (1975).

Rajagoplan, K., and D. Luss, "Influence of Catalyst Pore Size on Demetallation Rate," *Ind. Eng. Chem., Process Des. Dev.*, **18**, 459 (1979).

Richardson, R. L., and S. K. Alley, "Consideration of Catalyst Pore Structure and Asphaltenic Sulfur in the Desulfurization of Resids," *ACS Symp., Div. of Petro. Chem.*, Preprints, **20**, 554 (1975).

Satterfield, C. N., C. K. Cotton, and W. A. Pitcher, Jr., "Restricted Diffusion in Liquids within Fine Pores," *AIChE J.*, **19**, 628 (1973).

Satterfield, C. N., and G. W. Roberts, "Kinetics of Thiophene Hydrogenolysis on a Cobalt Molybdate Catalyst," *AIChE J.*, **14**(1), 159 (1968).

Sato, M., N. Takayama, S. Kurita, and T. Kwan, "Vanadium and Nickel Deposits Distribution in Desulfurization Catalyst," *Nippon Kagaku Zasshi*, **92**(10), 834 (1971).

Shah, Y. T., and J. A. Paraskos, "Intraparticle Diffusion Effects in Residue Hydrodesulfurization," *Ind. Eng. and Chem. Process. Des. Dev.*, **14**, 368 (1975).

Speight, J. G., *The Desulfurization of Heavy Oils and Residua*, Marcel Dekker, New York (1981).

Spry, J. C., and W. H. Sawyer, "Configurational Diffusion Effects in Catalytic Demetallization of Petroleum Feedstocks," Preprint 30C, 68th Annual AIChE Meeting, Los Angeles (Nov. 16-20, 1975).

Tamm, P. W., H. F. Harnsberger, and A. G. Bridge, "Effects of Feed Metals on Catalyst Aging in Hydroprocessing Residuum," *I & E Chem., Process. Des. Dev.*, **20**, 262 (1981).

Yen, T. F., J. G. Erdman, and S. S. Pollack, "Investigation of the Structure of Petroleum Asphaltenes by X-Ray Diffraction," *Anal. Chem.*, **33**, 1587 (1961).

Manuscript received February 16, 1983; revision received June 17, and accepted July 1, 1983.